

Supplemental data

MULTIVALENT BINDING OF FBP21-TANDEM-WW DOMAINS FOSTERS PROTEIN RECOGNITION IN THE PRE-SPLICEOSOME.

Stefan Klippel^{#1}, Marek Wieczorek^{#1}, Michael Schümann², Eberhard Krause², Berenice Marg³, Thorsten Seidel³, Tim Meyer⁴, Ernst-Walter Knapp⁴ & Christian Freund¹

snRNP core proteins	U4/U6	catalytic step 1 proteins	other splicing-related proteins
snRNPD1	U4/U6 snRNP 60 kDa	Prp19	BAT2
snRNPD2	U4/U6 snRNP 61 kDa		CA150
snRNPD3	U4/U6 snRNP 90 kDa	catalytic step 2 proteins	CHERP
snRNPE		RBM17	CREAP1
snRNPF	U4/U6.U5	RNPS1	DDX5
snRNPG	U4/U6.U5 snRNP 110 kDa	RNA-processing	DDX46
	HSPC006	CPSF25	LSM11
U1		CPSF6	NONO
snRNP70	U5	CPSF7	PTBP1
U1C	U5 snRNP 100 kDa (DDX23)	DDX1	PUF60
	U5 snRNP 102 kDa	DDX3	RBM10
U2	U5 snRNP 116 kDa	DDX30	RBM14
SF3A1	U5 snRNP 200 kDa	DDX36	RBM25
SF3A2	U5 snRNP 220 kDa (PrpF8)	MATR3	RBM39
SF3A3		MOV10	RED
SF3B1	hnRNPs	PAB1	SF1
SF3B2	HNRPC	PABPC4	SF4
SF3B3	HNRPD		SFPQ
SF3B4	HNRPF	assembly-related	SFRS3
SF3B5	HNRPG (RBMX)	DDX15	SFRS6
SF3B14	HNRPH	hPrp19	SFRS8
	HNRPM	HRMT1L5	SFRS15
SMN-complex	HNRPQ	SF1	SKIV2L2
Gemin3	HNRPR	SRm300	SRPK1
Gemin4	HNRPU	SRPK2	SR140
Gemin5	HNRPUL1		SRRM2
PRMT5			STIP
			UPF1
			WBP11
			YB1

Figure S1. Spliceosomal proteins interacting with FBP21-tandem-WW as identified by SILAC-MS.

SILAC experiments were performed as described in experimental procedures. Molecules that belonged to the hundred most highly enriched proteins in these pulldown experiments are depicted in black while proteins which were found in the pulldown but were only moderately enriched are depicted in gray.

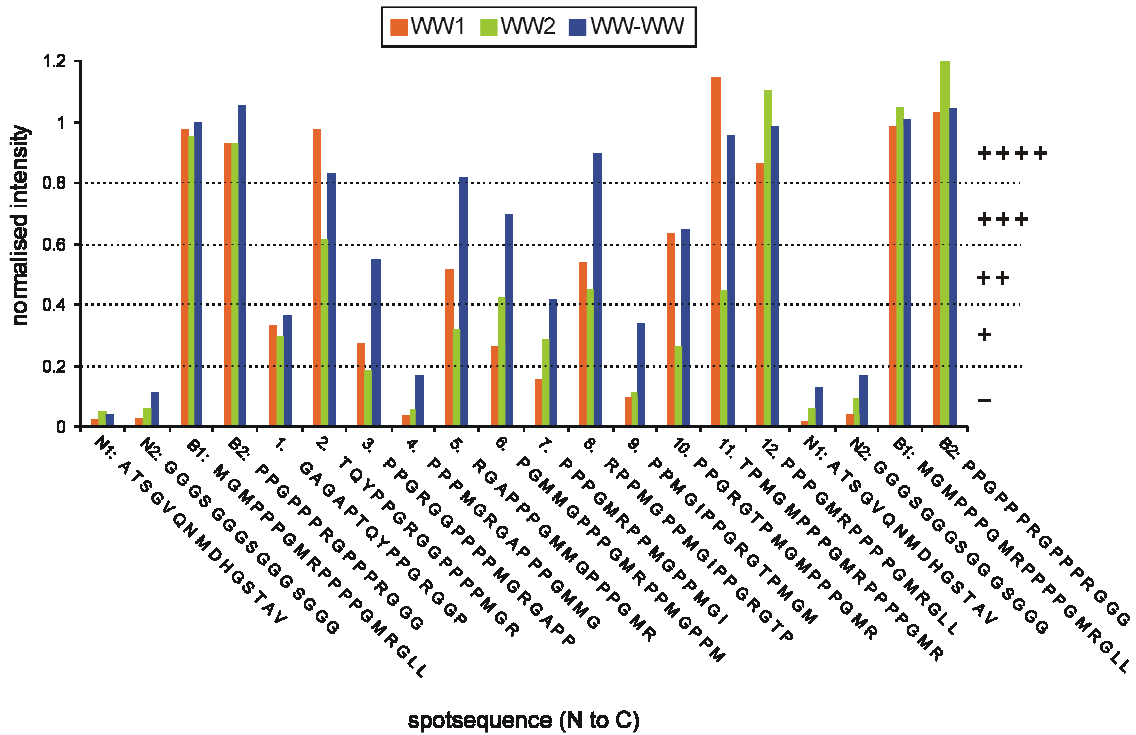


Figure S2. Peptide SPOT experiments to classify relative affinities of the FBP21 single domains and tandem domain along the PRS containing SmB-tail region.

Peptides with an overlapping sequence of 15-18 amino acids derived from the SmB tail (aa 163-231) were spotted onto a cellulose membrane and incubated either with GST fusions of WW1, WW2 or tandem-WW. In case of the tandem-WW domains we observed moderate to strong binding for all peptides except peptide 4 (no binding) and 9 (weak binding). Considering that the spotted sequences contain an overlap of 10-13 amino acids we can exclude a single preferred binding site. Qualitatively, relative affinities for individual sequences of the SmB-tail are comparable for WW1, WW2 and tandem-WW indicating that all three constructs exert similar binding specificity (control motifs: B/binder; N/non-binder).

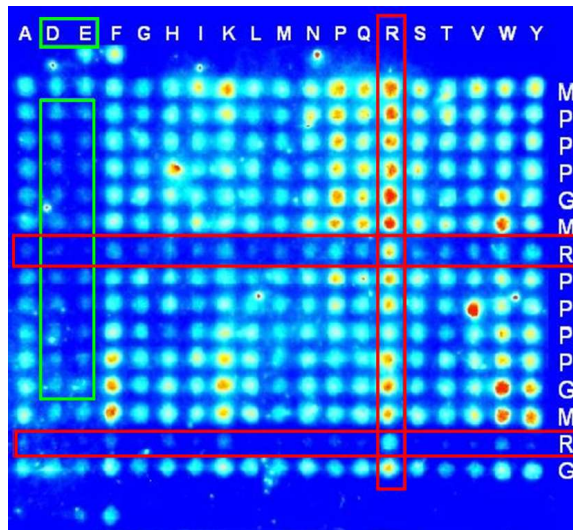


Figure S3. Substitution analysis of a bivalent SmB ligand in interaction with FBP21-tandem-WW by SPOT analysis.

Single amino acid replacements of each residue of a shortened SmB-2 peptide (SmB aa 218-231) were probed by GST-FBP21-tandem-WW as described in the experimental procedures. Most strikingly, substitution of the arginine leads to a prominent reduction in signal intensity indicating a reduced affinity (red horizontal mark). On the other hand the binding strength could be enhanced by introducing an additional arginine residue at different positions (red vertical mark). The importance of the positive charge is underlined by the finding, that the introduction of a negative charge (aspartic acid, glutamic acid) within the ligand reduces the affinity (green mark).

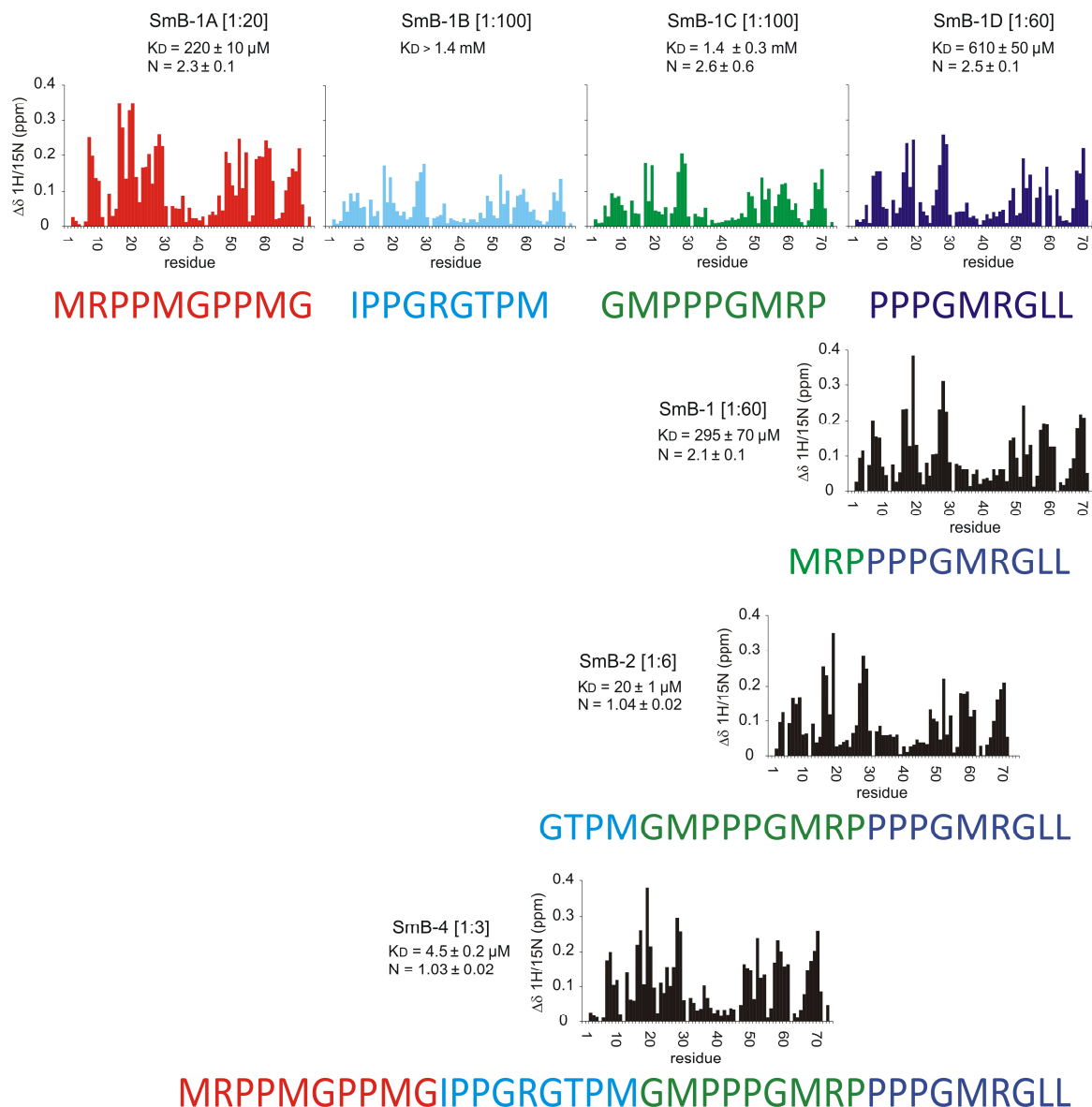


Figure S4. Chemical shift perturbations and K_D values (ITC) of the FBP21-tandem-WW domains upon binding SmB ligands with a different number of PRS. SmB-4 was divided into four non-overlapping peptides (SmB-1A-D). Affinities were measured by ITC and K_D values and stoichiometries determined when possible. The addition of three residues (“MRP”) at the N-terminus of SmB-1D enhances the affinity by a factor of two as shown for SmB-1. The stoichiometry is approximately two arguing that the two WW domains in the tandem-WW construct each interact with an individual peptide. SmB-2 comprises two PRS motifs and allows for a bivalent interaction ($N=1$) while SmB-4 possesses four potential PRM motifs (see also Figure 2 in the main text). The higher ligand valency in SmB-4 leads to an additional affinity enhancement while the stoichiometry remains $N=1$. Residues affected by ligand binding are mainly located within the three beta-sheets of WW1 and WW2 and are part of the known interface for monovalent WW:PRS interactions.

SmB-4: MRPPMGPPMGIPPGRGTPMGMPPPGMRP PPPGMRGLL

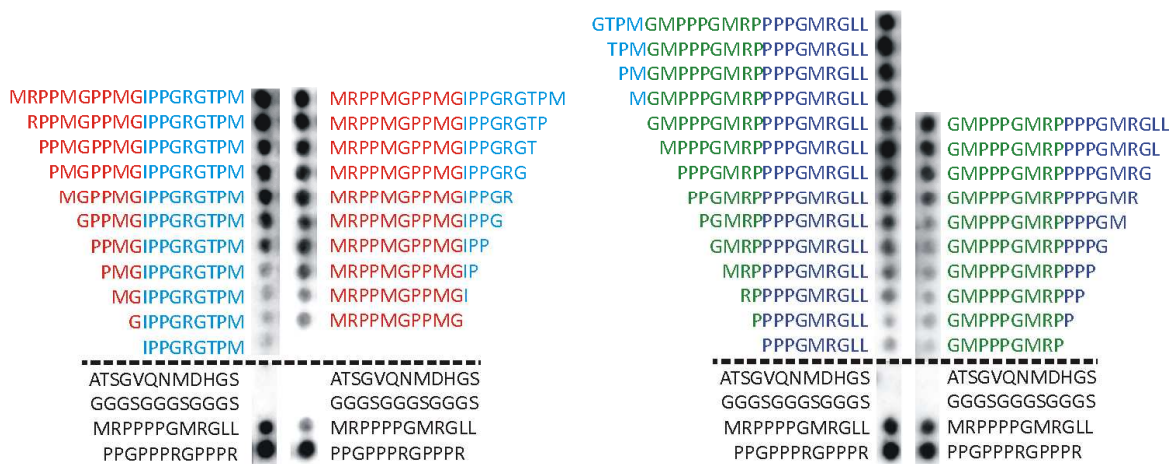


Figure S5. SPOT analysis of truncation experiment of bivalent SmB ligands derived from aa 195-231 of SmB. Bivalent SmB peptides were shortened by individual amino acids starting from either the N or C terminus and incubated with the GST-FBP21-tandem-WW domain. The truncation of one PRS motif leads to a decreased signal intensity implicating a loss of affinity based on the transition from a bivalent to a monovalent interaction. A similar pattern was observed in a substitution analysis where peptide residues were replaced by alanine-serine (Ala₄Ser) stretches (data not shown). Positive and negative controls are shown below the dotted line (from top to bottom: non-binder, non-binder, binder, binder).

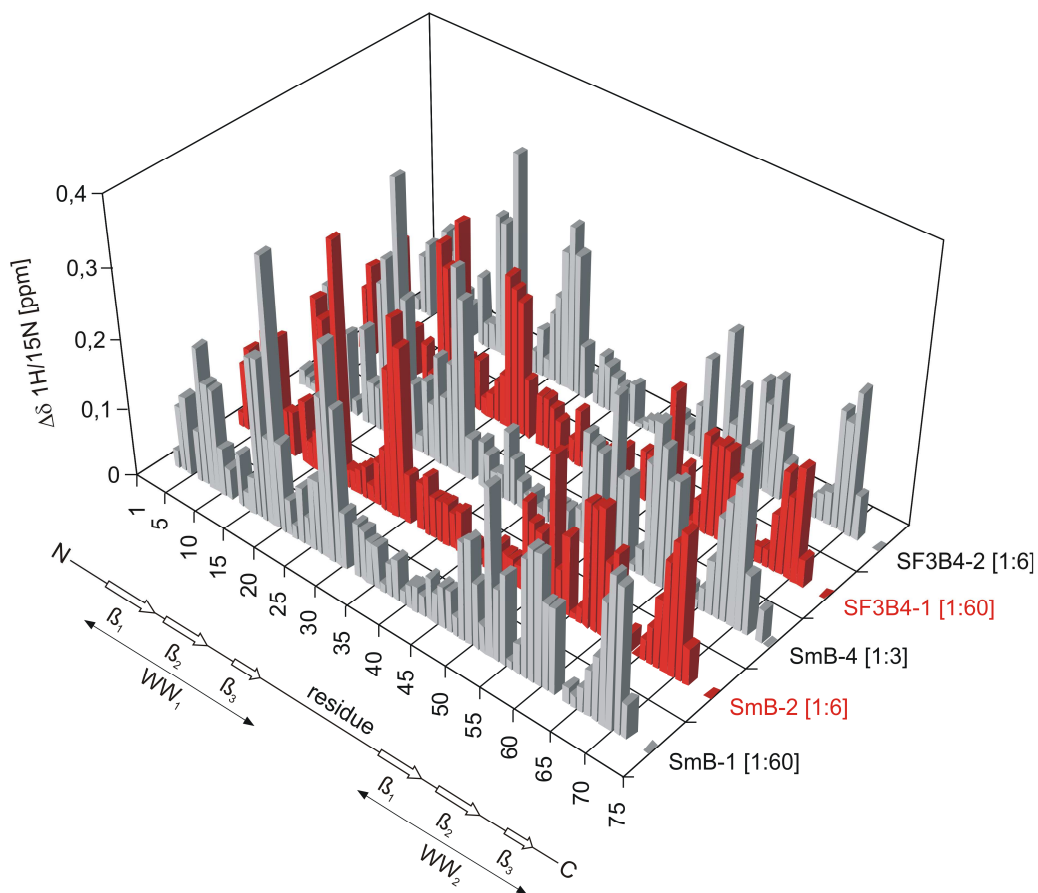


Figure S6. Chemical shift perturbations of the FBP21-tandem-WW domains upon binding ligands with a different number of PRS.

Figure S6 shows a mapping of weighted chemical shifts for NH backbone resonances after saturation with SmB (1, 2 or 4 motifs) and SF3B4 (1 or 2 motifs) ligands. Residues affected by ligand binding are mainly located within the three beta-sheets of WW1 and WW2 and are part of the known interface for monovalent WW:PRS interactions. Only subtle differences are observed between ligands of different valency.

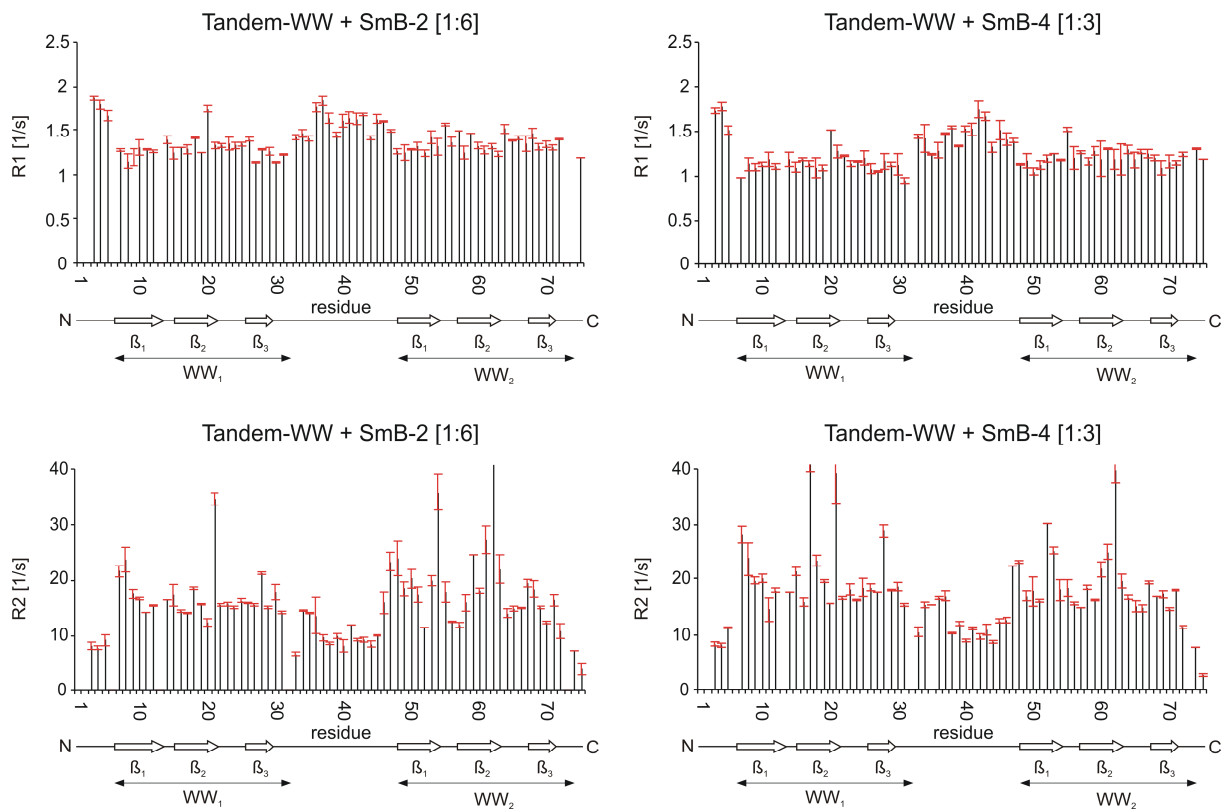


Figure S7. ^{15}N Relaxation rates for the FBP21-tandem-WW domain in complex with SmB-2 (left) and SmB-4 (right). ^{15}N - ^1H R1 and R2 rates were measured at 750 MHz indicate a slightly higher flexibility and mobility for the linker region compared to the WW-domains in both complexes. Correlation times of the tandem-WW domain in complex with SmB-2 (8 ± 0.3 ns) and SmB-4 (9 ± 0 ns) were calculated from T1/T2 ratios and are in agreement with the molecular weight of a 1:1 binding mode in both cases (tandem-WW + SmB-2: 11 kDa, tandem-WW + SmB-4: 12.5 kDa).